Electronic Supplementary Material (ESI) for New Journal of Chemistry.

Supporting Information

Uniform nickel-cobalt nanoparticles embedded nitrogen-doped carbon nanofibers for highly active and durable oxygen reduction electrocatalysts

Jingyu Song[a‡], Xuan Xie[a‡], Kanjun Sun[b], Mingxin Zhang[a], Haikuo Lei[a], Hui Peng[a], Guofu Ma*[a]*

[a]Key Laboratory of Eco-functional Polymer Materials of the Ministry of Education, Key Laboratory of Polymer Materials of Gansu Province, College of Chemistry and Chemical Engineering, Northwest Normal University, Lanzhou 730070, China.

[b] College of Chemistry and Chemical Engineering, Lanzhou City University, Lanzhou 730070, China.

‡These authors contributed equally to this work. They should thus be considered co-first authors.

*Corresponding authors. E-mail addresses: penghui@nwnu.edu.cn (H. Peng), magf@nwnu.edu.cn (G. Ma)

S1. Materials characterizations

The morphology and microstructure of the as-prepared carbon materials were examined by field emission scanning electron microscopy (FE-SEM, Carl Zeiss-Ultra Plus, Germany) and transmission electron microscopy (TEM, FEI Tecnai G2 F20 S-Twin, USA). The crystallographic structure of the materials was determined by X-ray diffraction (XRD, D/Max-2400, Rigaku) equipped with CuKα radiation (k = 1.5418 Å). Raman spectra were collected on an in Via Raman spectrometer (Rainie Salt Public Co. Ltd., Britain) with a laser wavelength of 514 nm. The elemental (C, O, N, Co, Ni and P) microanalysis was carried out using the Elemental Analyzer Vario EL. X-ray photoelectron spectroscopy (XPS) measurement was performed on an Escalab 210 system (Germany) with Al Kα radiation source. The Brunauer-Emmett-Teller (BET) surface area of the samples was analyzed by nitrogen adsorption-desorption in a surface area and porosimetry analyzer (ASAP 2020, Micromeritics, U.S.A.).

Calibration of RHE electrode:

In this work, Hg/HgO (1 M KOH solution) electrode was used as reference electrode for all measurements. All measured potentials were calibrated to the reversible hydrogen electrode (RHE) as described in literature at 25^{o}C. The calibration was conducted with a standard three-electrode system in the highly pure hydrogen saturated 0.1 M KOH solution. Two polished Pt wire were used as the counter and working electrodes, respectively. The thermodynamic potential was determined by cyclic voltammetry (CV) and linear scanning voltammetry (LSV) scan at a scan rate of 1 mV s^{-1}. The potential at zero current was regarded as the thermodynamic potential for the hydrogen electrode reactions.

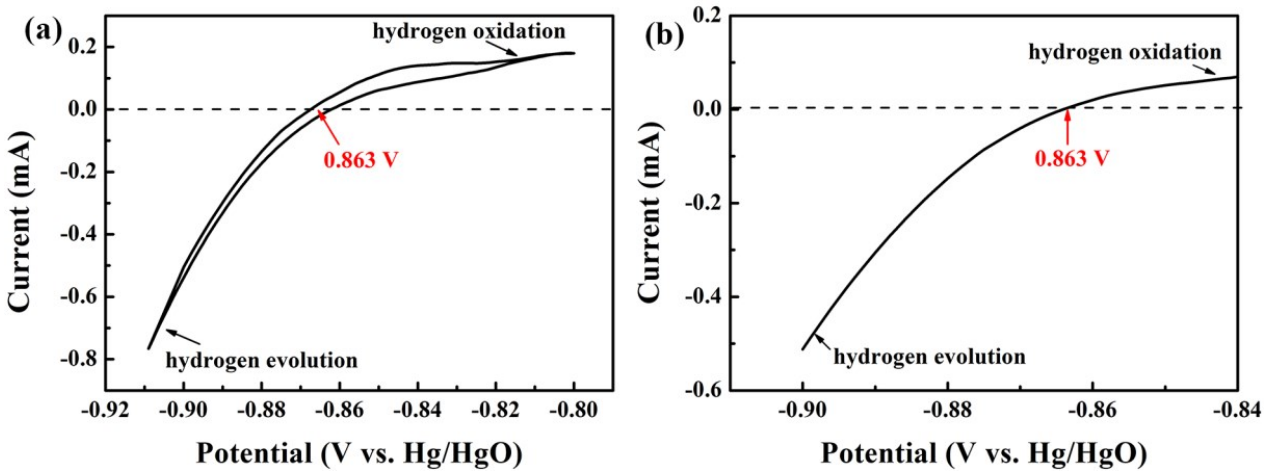

In 0.1 M KOH solution, the zero current point is at -0.863 V, so E(RHE) = E(Hg/HgO) + 0.863.

S2. Electrochemical measurements

All ORR performance date using a rotating disk electrode (RDE, PINE Research Instrumentation) with an Autolab bipotentiostat (Model PGSTAT128N) workstation at ambient temperature. All test was carried out using a three-electrode system, a Pt wire as counter electrode, Hg/HgO (1 M KOH) as reference electrode and glassy carbon (GC) disk electrode (5 mm in diameter) are used as the working electrodes.

The preparation of the working electrode is as follows: 5 mg catalysis was added to 1 ml Nafion/enthol and ultrasonic dispersion for 30 min. Measuring 8 μl drop onto the working electrode and waiting for natural dry (The catalyst loading is 0.2038 mg cm^{-2}). Before tests, 0.1 M KOH solution should be saturated with N_2/O_2.

Calculate kinetic current density (J_k) and electronic transfer number (n) according to the equation Koutecky-Levich given below:

$$\frac{1}{J} = \frac{1}{J_k} + \frac{1}{B\omega^{1/2}} \qquad (1)$$

$$B = 0.2nFD_0^{2/3}V^{-1/6}C_0 \qquad (2)$$

where J and J_k are the measured current density and the kinetic current density, respectively. ω is the

electrode rotation speed, B could be determined from the slope of the K-L plots, n is the number of electrons transferred per oxygen molecule, F is the Faraday constant (96485 C mol^{-1}), D_0 is the diffusion coefficient of O_2 (1.9×10^{-5} cm^2 s^{-1}), V is the kinetic viscosity (0.01 cm^2 s^{-1}), and C_0 is the concentration of O_2 (1.2×10^{-6} mol cm^{-3}).

For the RRDE tests, the n and hydrogen peroxide yield ($\%H_2O_2$) were calculated by the following equations:

$$n = \frac{4I_D}{I_D + (I_R / N)} \quad (3)$$

$$\%H_2O_2 = \frac{200I_R / N}{I_D + (I_R / N)} \quad (4)$$

where I_D is the disk current, I_R is the ring current, N (37%) is the current collection coefficient at the Pt ring.

Fabrication of Zn-air batteries: Primary Zn-air batteries were fabricated and evaluated at ambient conditions. Typically, a polished Zn foil (0.2 mm thickness) was employed as the anode. The air electrode was prepared by drop-casting as-prepared catalyst ink onto hydrophobic carbon paper (Fuel Cell Store, effective area = 2 cm^{-2}), yielding a catalyst loading of 1.0 mg cm-2. Waterproof and breathable membrane and Ni foam were used as gas diffusion layer (GDL) and current collector, respectively. The electrolyte was 6 M KOH aqueous solutions. The discharge polarization curve was recorded by LSV at a scan rate of 5 mV s^{-1} on an Autolab electrochemical workstation. The specific capacity (mAh g^{-1}) of $Ni_{0.5}Co_1$@NCNFs and Pt/C were calculated based on the following equations[2]:

$$\text{Specific capacity} = \frac{\text{discharge current} \times \text{working time}}{\text{mass of consumed zinc}} \quad (5)$$

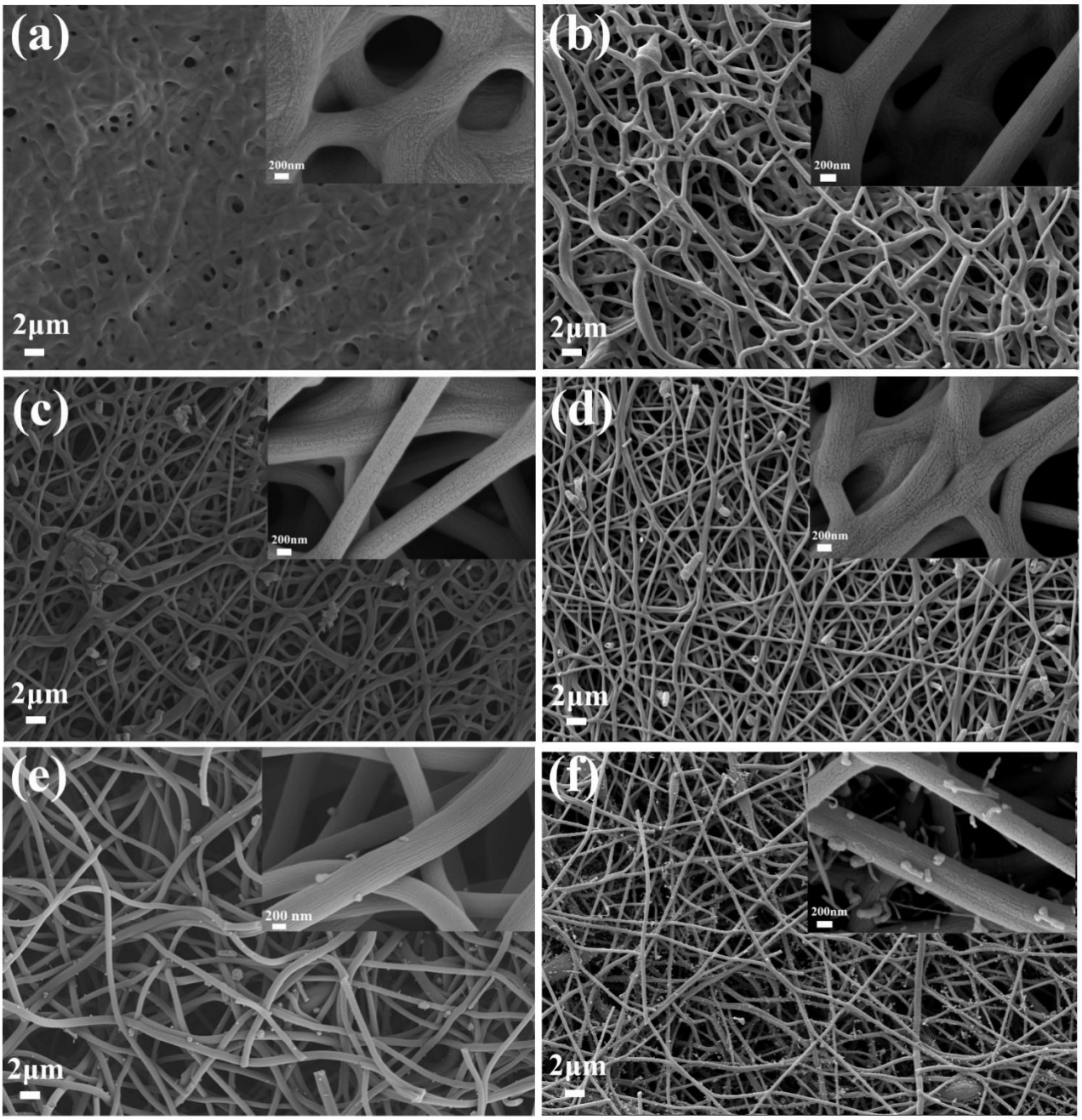

Fig. S1 SEM image of (a) NCNFs; (b) $Ni_{0.5}$@NCNFs; (c) Co_1@NCNFs; (d) $Ni_{0.5}Co_{0.5}$@NCNFs; (e) $Ni_{0.5}Co_1$@NCNFs, (f) $Ni_{0.5}Co_{1.5}$@NCNFs.

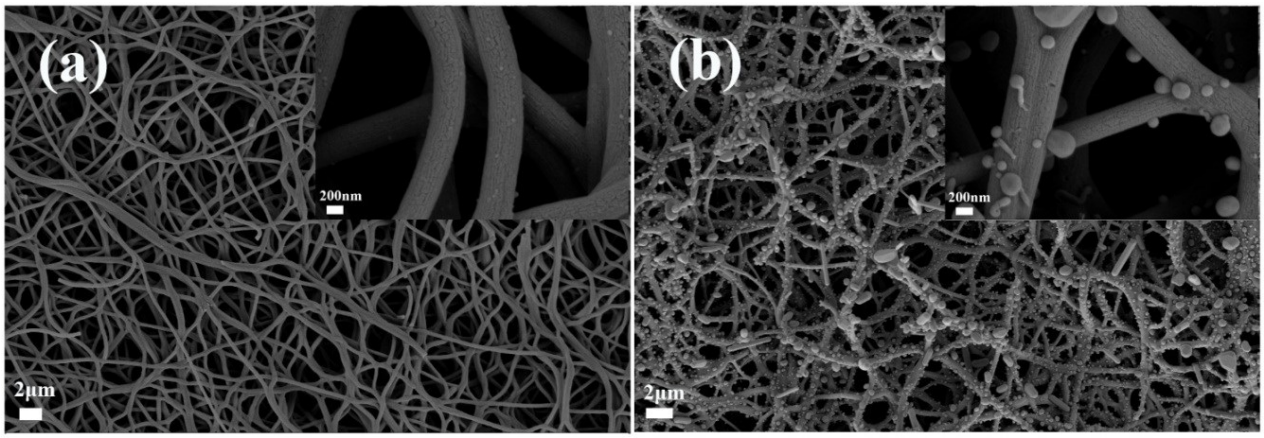

Fig. S2 SEM image of (a) $Ni_{0.5}Co_1$@NCNFs-800; (b) $Ni_{0.5}Co_1$@NCNFs-1000.

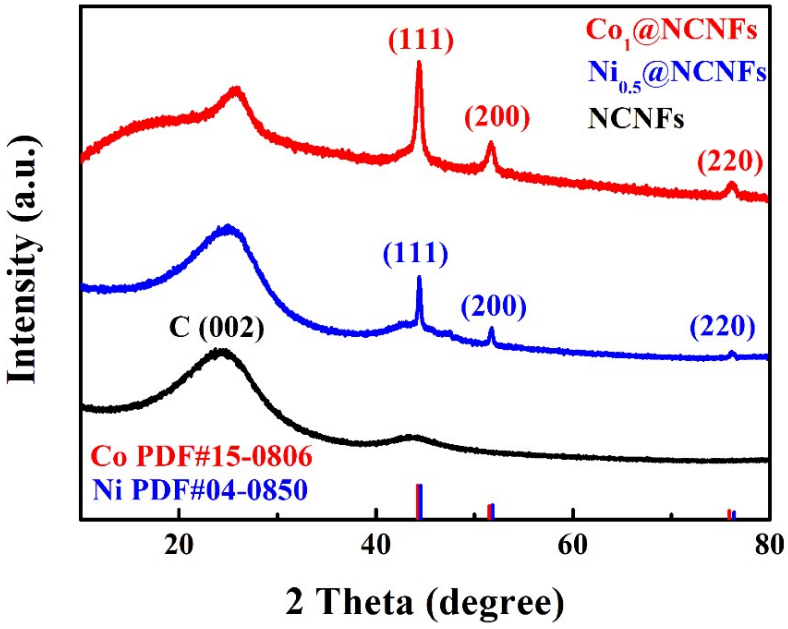

Fig. S3 XRD pattern of NCNFs, $Ni_{0.5}$@NCNFs and Co_1@NCNFs.

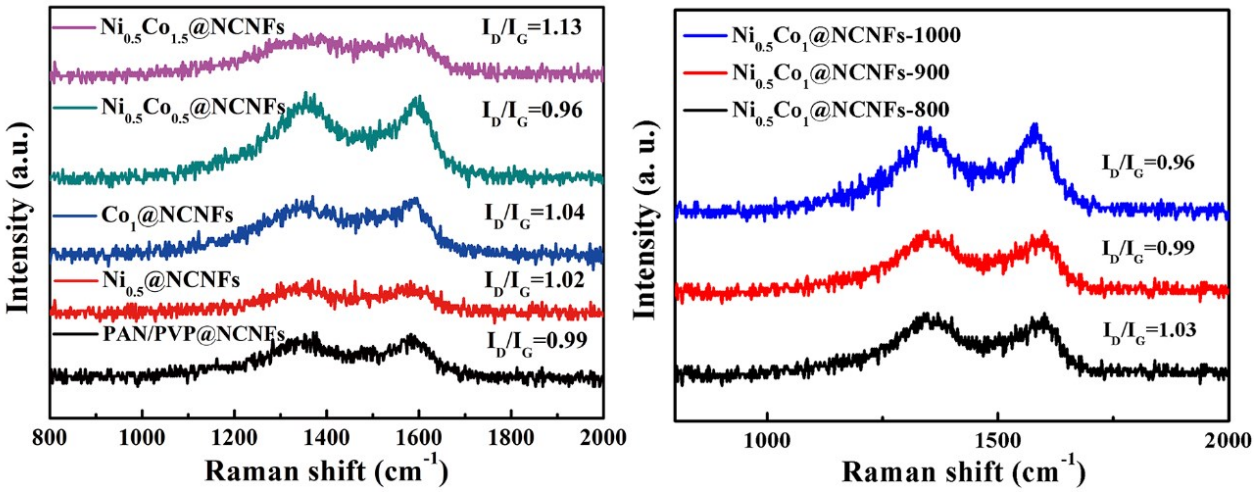

Fig. S4 (a) Raman spectra of NiCo@NCNFs carbonized at different mole ratio of Ni^{2+}/Co^{2+} and $Ni_{0.5}Co_1$@NCNFs carbonized at different carbonization temperatures.

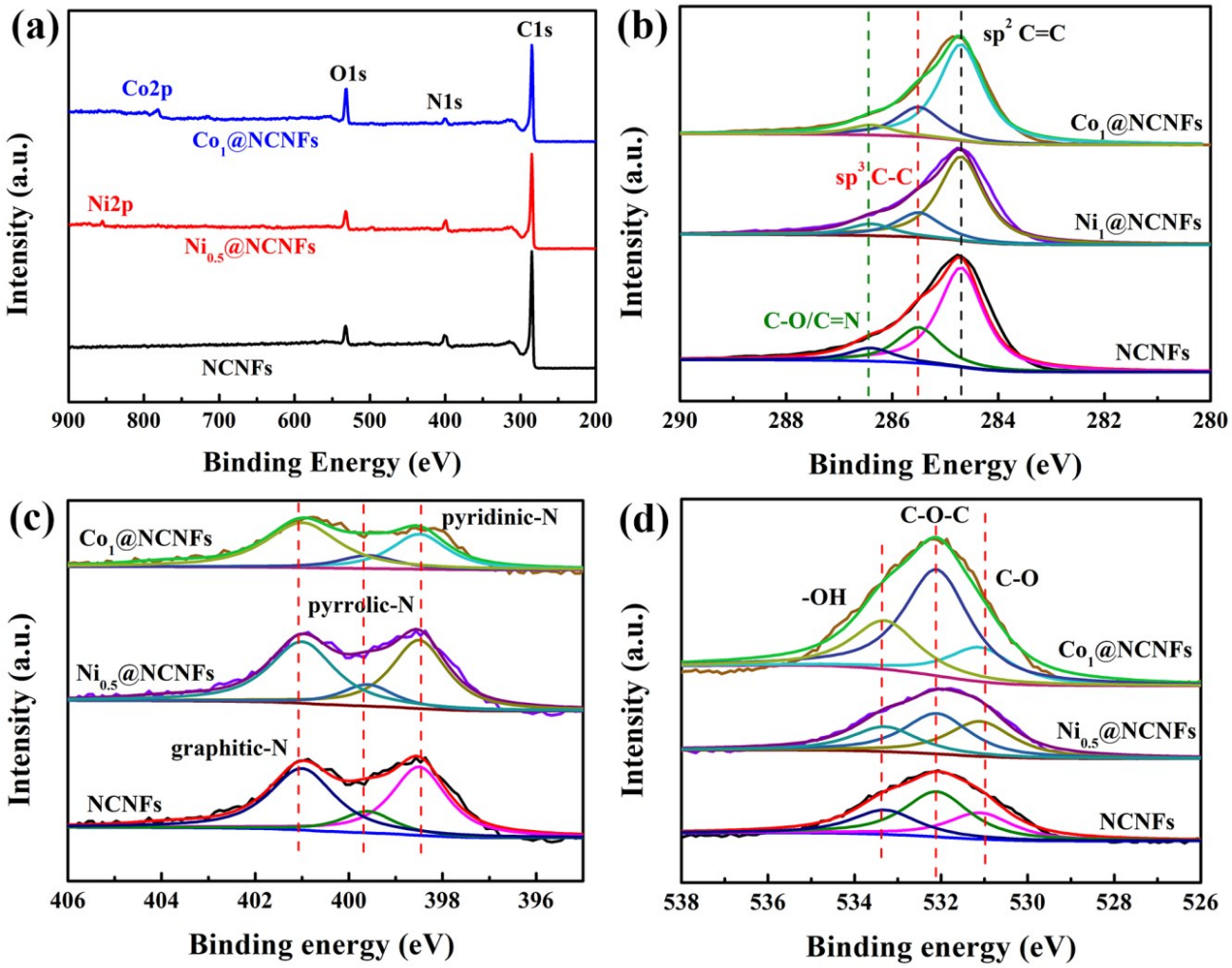

Figure S5. XPS survey spectra (a) of NCNFs, $Ni_{0.5}$@NCNFs and Co_1@NCNFs, High-resolution XPS spectra of (b) C1s, (c) N1s and (d) O1s.

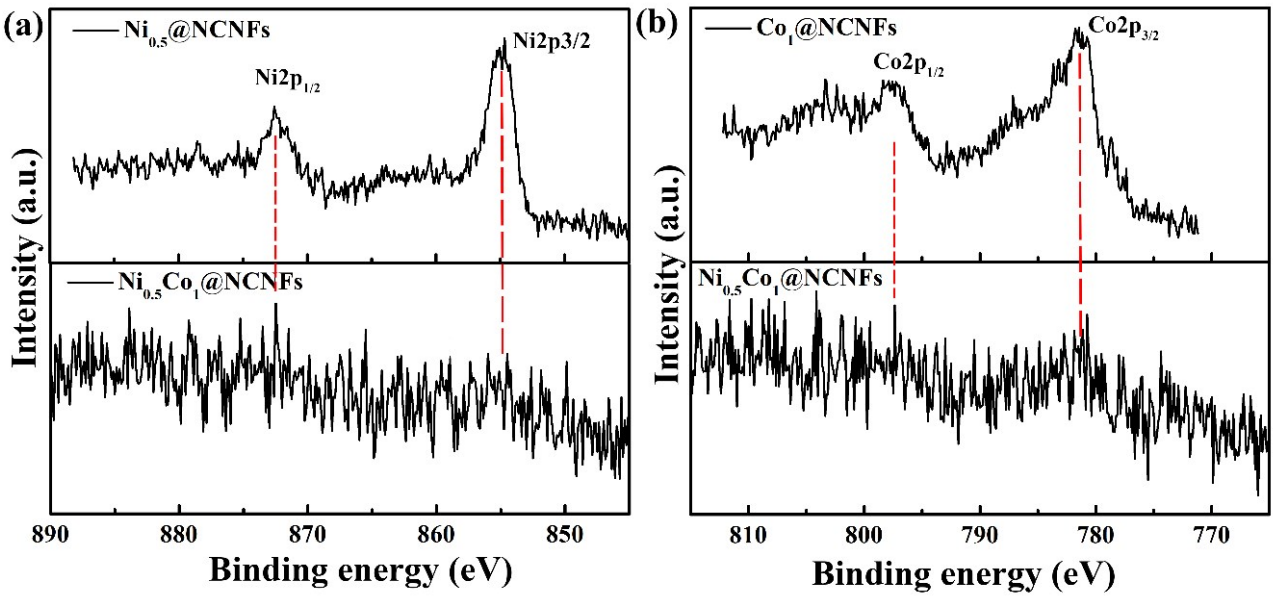

Fig. S6 XPS characterization of $Ni_{0.5}$@NCNFs, Co_1@NCNFs and $Ni_{0.5}Co_1$@NCNFs (a) Ni2p, (b) Co2p.

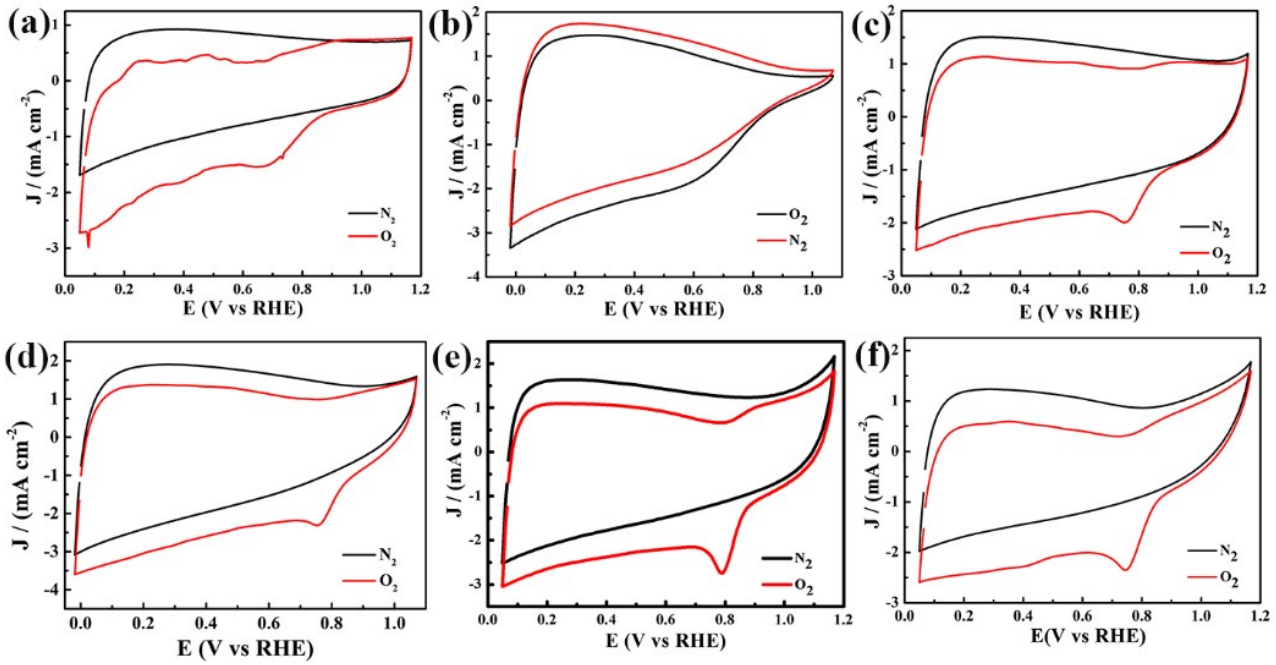

Fig. S7 CV curves of NCNFs and NiCo@NCNFs electrocatalysts in O_2-saturated 0.1 M KOH (scan rate: 50 mV s^{-1}).

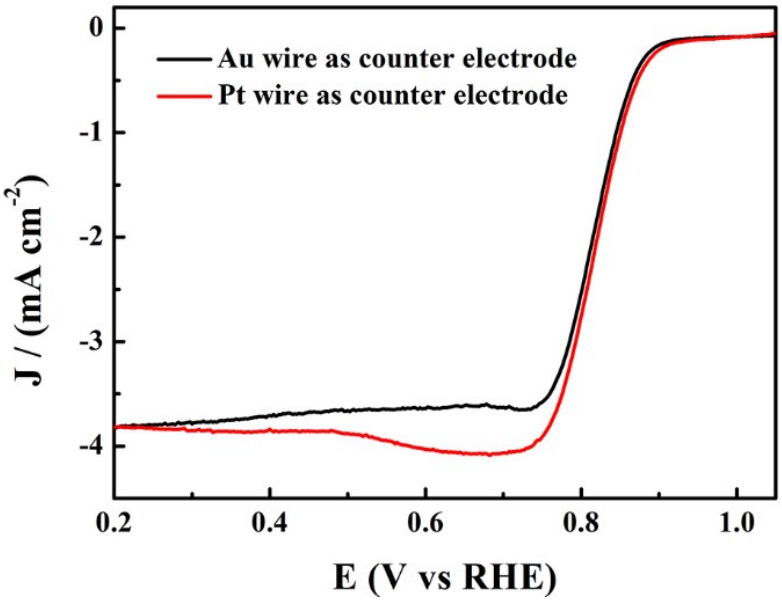

Fig. S8 LSV curve of $Ni_{0.5}Co_1$ @NCNFs in O_2-saturated 0.1 M KOH using the different counter electrode.

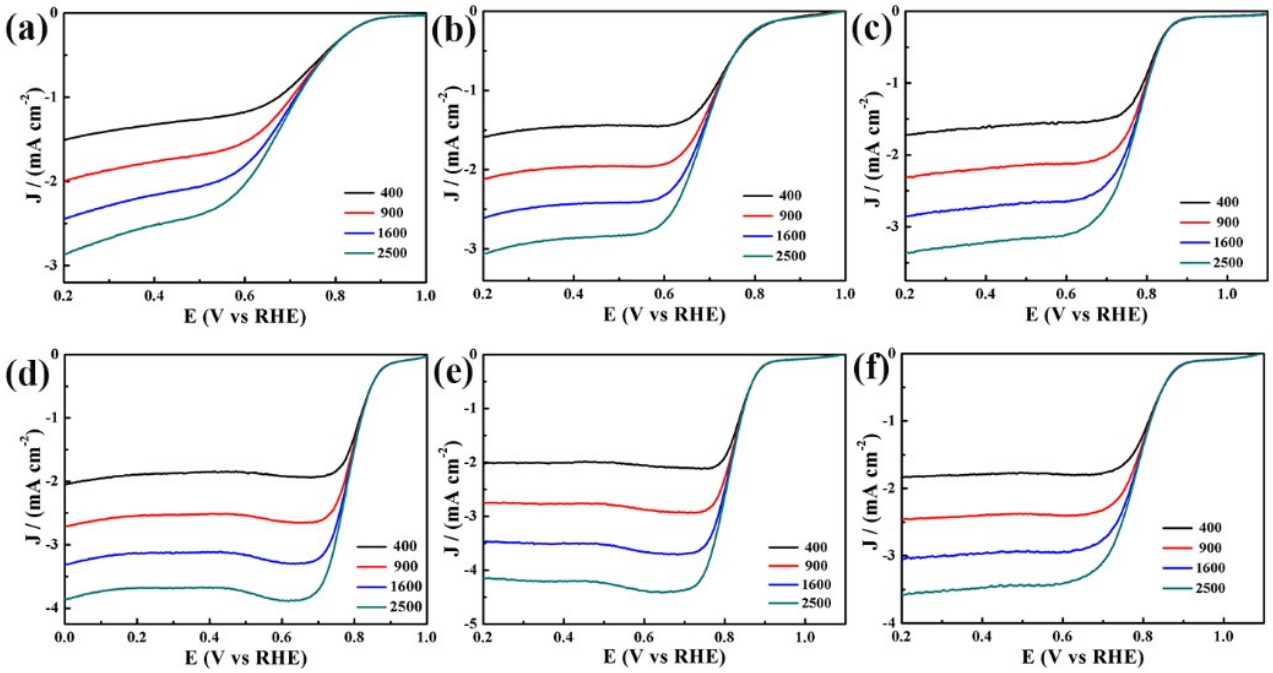

Fig. S9 LSV curves of (a) NCNFs; (b) $Ni_{0.5}$@NCNFs; (c) Co_1@NCNFs; (d) $Ni_{0.5}Co_{0.5}$@NCNFs; (e) $Ni_{0.5}Co_1$@NCNFs; (f) $Ni_{0.5}Co_{1.5}$@NCNFs in O_2-saturated 0.1 M KOH (scan rate: 5 mV s^{-1}) with various rotation rates.

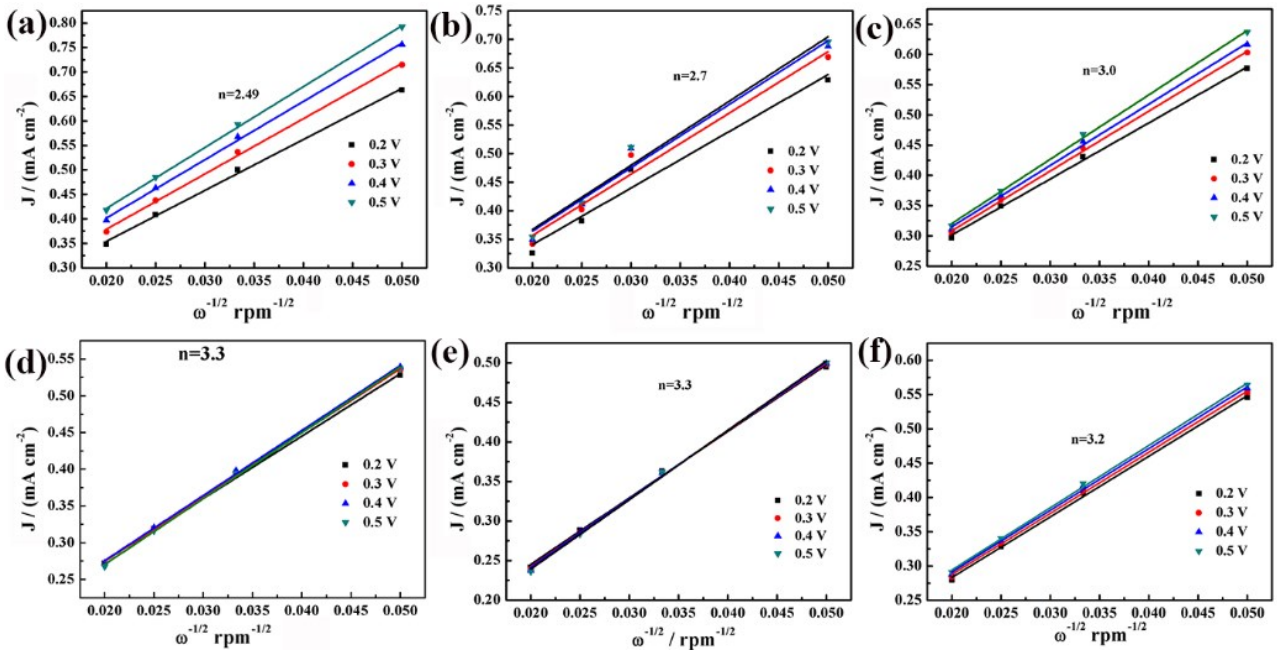

Fig. S10 The K-L plots of (a) NCNFs; (b) $Ni_{0.5}$@NCNFs; (c) Co_1@NCNFs; (d) $Ni_{0.5}Co_{0.5}$@NCNFs; (e) $Ni_{0.5}Co_1$@NCNFs; (f) $Ni_{0.5}Co_{1.5}$@NCNFs at different potentials.

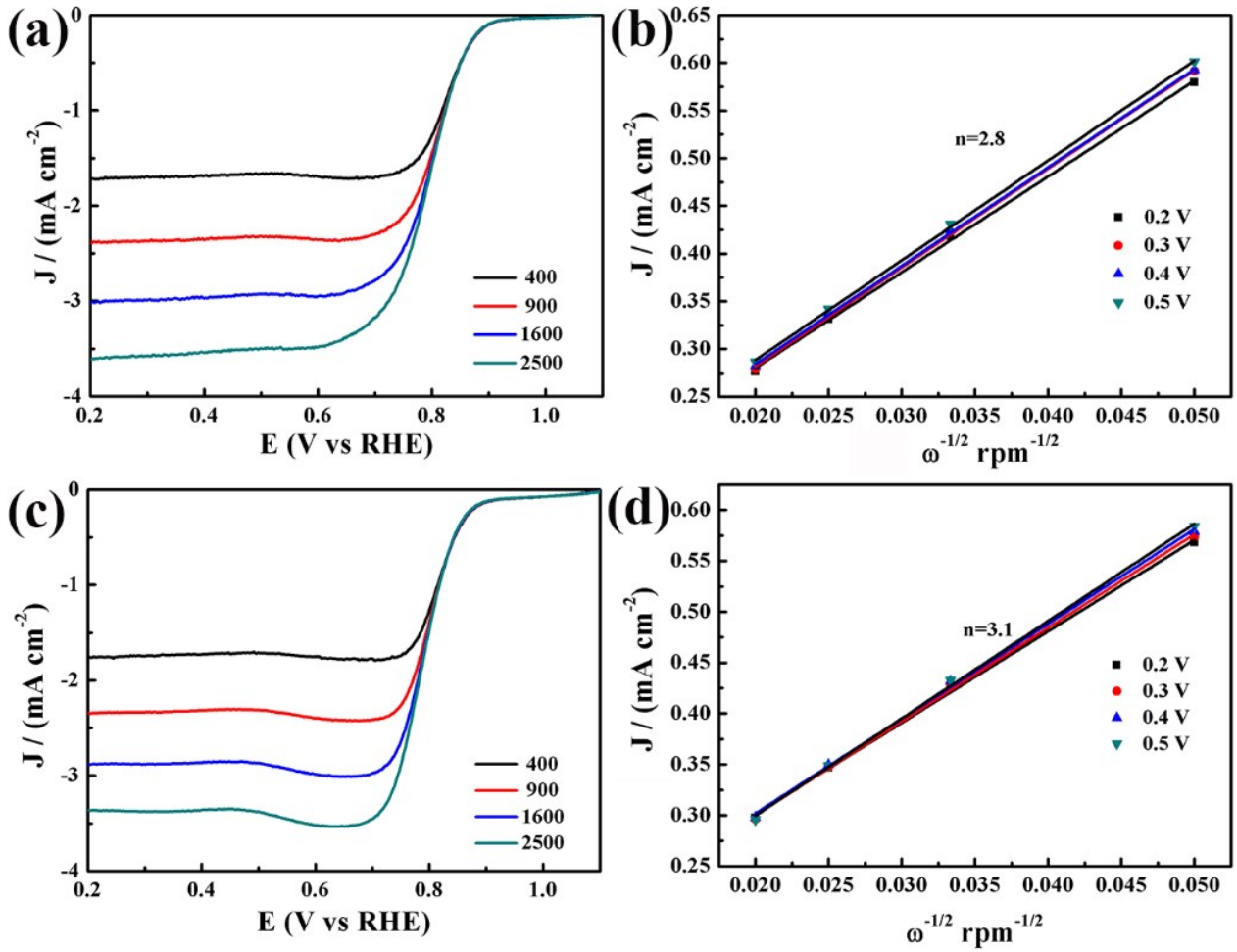

Fig. S11 (a) $Ni_{0.5}Co_1$@NCNFs-800 in O_2-saturated 0.1 M KOH (scan rate: 50 mV s^{-1}) with various rotation rates. The K-L plots of (b) $Ni_{0.5}Co_1$@NCNFs-800. (c) $Ni_{0.5}Co_1$@NCNFs-1000 in O_2-saturated 0.1 M KOH (scan rate: 50 mV s^{-1}) with various rotation rates. The K-L plots of (d) $Ni_{0.5}Co_1$@NCNFs-1000.

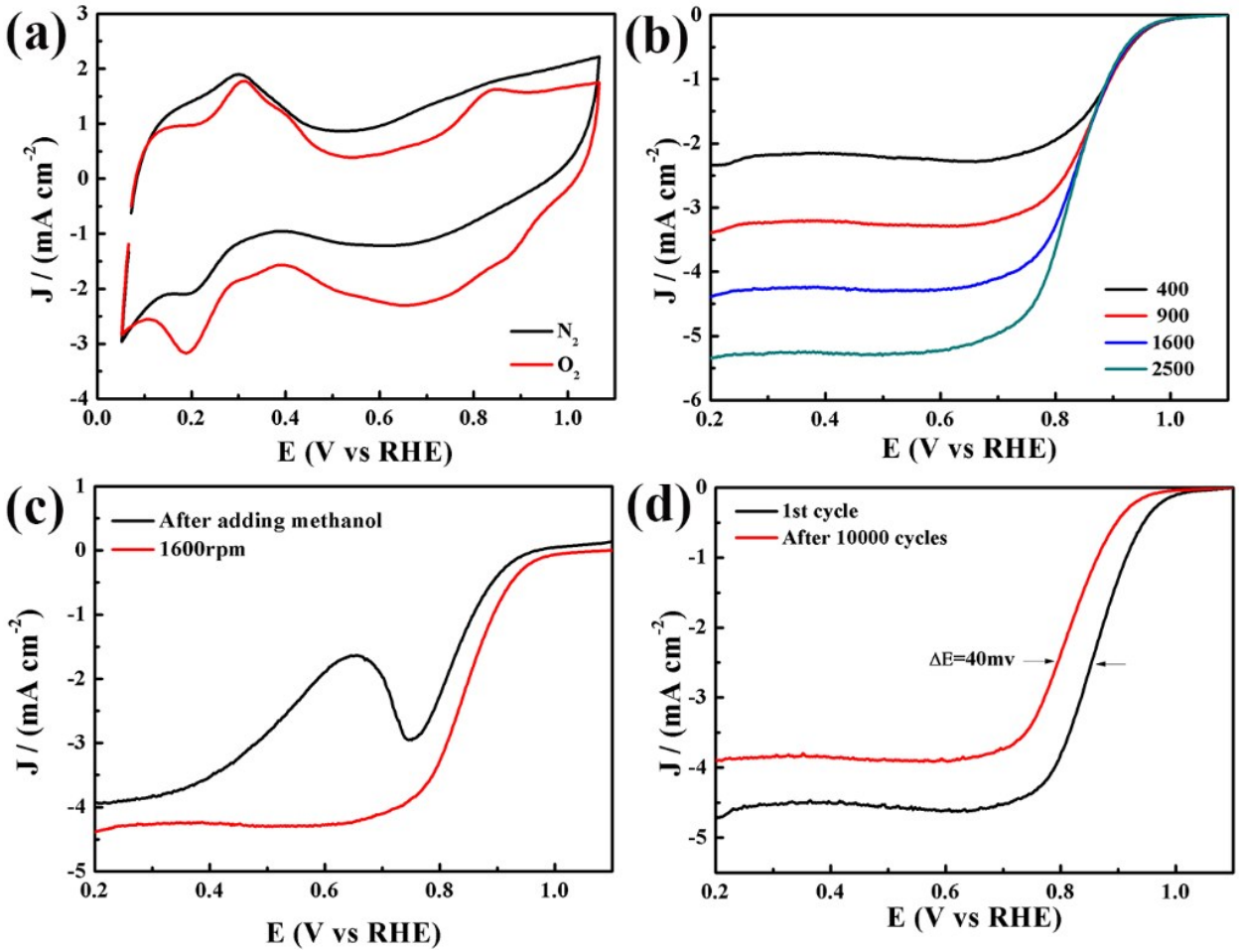

Fig. S12 (a) CV curves of 20% Pt/C in N_2-saturated and O_2-saturated 0.1 M KOH (scan rate: 50 mV s^{-1}). (b) LSV curves of 20% Pt/C in O_2-saturated 0.1 M KOH (scan rate: 50 mV s^{-1}) with various rotation rates. (c) ORR polarization curves of 20% Pt/C in O_2-saturated 0.1 M KOH with and without 0.5 M CH_3OH at 1600 rpm. (d) ORR polarization curve before and after 10000 cycles of the 20% Pt/C.

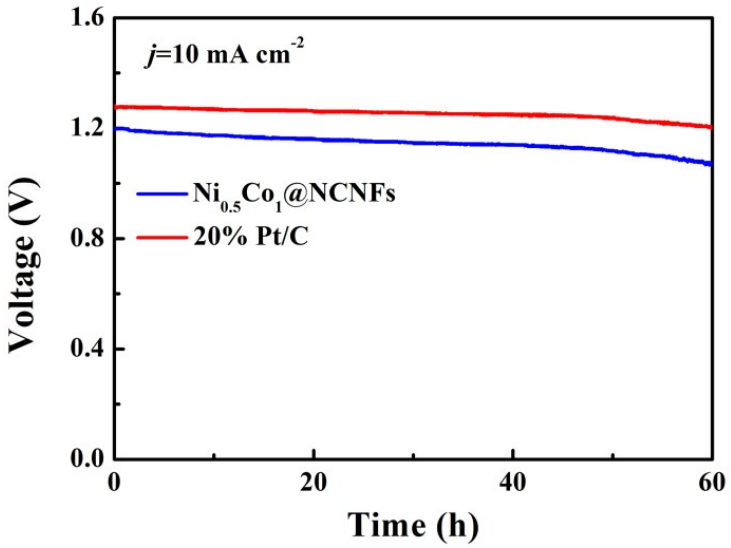

Fig. S13. Long time galvanostatic discharge curves of a Zn-air battery.